



Brain activity dynamics after traumatic brain injury indicate increased state transition energy and preference of lower order states

Nate Roy^{a,*}, S. Parker Singleton^b, Keith Jamison^b, Pratik Mukherjee^c, Sudhin A. Shah^b, Amy Kuceyeski^b

^a Cornell University, Ithaca, NY, USA

^b Weill Cornell Medicine, New York, NY, USA

^c University of California, San Francisco, San Francisco, CA, USA

ARTICLE INFO

Keywords:

fMRI
Network Control Theory
TBI
Longitudinal
Structural connectome
Cognition

ABSTRACT

Traumatic Brain Injury (TBI) can cause structural damage to the neural tissue and white matter connections in the brain, disrupting its functional coactivation patterns. Although there are a wealth of studies investigating TBI-related changes in the brain's structural and functional connectomes, fewer studies have investigated TBI-related changes to the brain's dynamic landscape. Network control theory is a framework that integrates structural connectomes and functional time-series to quantify brain dynamics. Using this approach, we analyzed longitudinal trajectories of brain dynamics from acute to chronic injury phases in two cohorts of individuals with mild and moderate to severe TBI, and compared them to non-brain-injured, age- and sex-matched control individuals' trajectories. Our analyses suggest individuals with mild TBI initially have brain activity dynamics similar to controls but then shift in the subacute and chronic stages of the injury (1 month and 12 months post-injury) to favor lower-order visual-dominant states compared to higher-order default mode dominant states. We further find that, compared to controls, individuals with mild TBI have overall decreased entropy and increased transition energy demand in the sub-acute and chronic stages that correlates with poorer attention performance. Finally, we found that the asymmetry in top-down to bottom-up transition energies increased in subacute and chronic stages of mild TBI, possibly indicating decreased efficacy of top-down inhibition. We replicate most findings with the moderate to severe TBI dataset, indicating their robustness, with the notable exception of finding the opposite correlation between global transition energy and mean reaction time (MRT). We attribute differences to the cohorts' varied injury severity, with perhaps a stronger compensatory mechanism in moderate to severe TBI. Overall, our findings reveal shifting brain dynamics after mild to severe TBI that relate to behavioral measures of attention, shedding light on post-injury mechanisms of recovery.

1. Significance statement

Using Network Control Theory (NCT), we analyze longitudinal changes in brain dynamics over the acute to chronic stages of mild and moderate to severe TBI. NCT modeling provides a framework for understanding how damage to structural white matter connections after TBI may alter patterns of functional brain activation, and, further, how these changes relate to impairment and recovery. We found that there was a shift in both the subacute and chronic stages of TBI to prefer lower-order (visual network) compared to higher-order (default mode network) states. In parallel, the overall amount of energy needed to transition between brain states was correlated with mean reaction time

on the Attention Network Test (ANT). Finally, we found an increase in the amount of energy needed to complete top-down relative to bottom-up transitions, suggesting decreased efficacy of top-down inhibition. This work is the first to use NCT to analyze the longitudinal time course of brain dynamics from acute to chronic stages after TBI, and may point toward neurobiological mechanisms of injury and recovery.

2. Introduction

TBI causes approximately 2.5 million emergency department visits, 282,000 hospitalizations, and 56,000 deaths each year (Faul and Coronado, 2015). TBI can affect cognition, motor function and emotional processes both in acute and chronic stages after injury

* Corresponding author.

E-mail address: nr284@cornell.edu (N. Roy).

Nomenclature

General Abbreviations

AMI	Adjusted Mutual Information
ANT	Attention Network test
dMRI	diffusion magnetic resonance imaging
fMRI	functional magnetic resonance imaging
FC	Functional Connectome/Connectivity
HC	Healthy Control
MRT	Mean Reaction Time
NCT	Network Control Theory
ROI	Region of Interest
RSN	Resting State Network
SC	Structural Connectome/Connectivity
TBI	Traumatic Brain Injury
TR	Repetition Time

Brain state abbreviations

DMN+/-	Default Mode Network high/low amplitude activation
FPN+/-	Frontoparietal Network high/low amplitude activation
SOM+/-	Somatomotor Network high/low amplitude activation
SUB+/-	Subcortical Network high/low amplitude activation
VATSON+/-	Ventral Attention/Somatomotor high/low amplitude activation
VIS+/-	Visual Network high/low amplitude activation

(Machamer et al., 2022; Silverberg et al., 2020). The search for biomarkers in TBI that would allow identification and targeted treatment of individuals predisposed to post-concussion syndrome has been largely inconclusive. TBI is also linked to heightened risk for neurodegenerative conditions such as Alzheimer's Disease, Parkinson's Disease, and chronic traumatic encephalopathy (VanItallie, 2019; Gardner and Yaffe, 2015; Petraglia et al., 2014). Thus, there exists a great, unmet need for proper neurobiological understanding of injury and recovery mechanisms that would in turn provide better diagnostic/prognostic, medical clearance and rehabilitation protocols for TBI. Without protocols that are informed by the underlying neurobiological mechanisms, populations such as athletes and military members remain at risk for repetitive TBI which only heighten the potential for long-term consequences (McAllister and McCrea, 2017; Dixon, 2017; Guskiewicz and Broglio, 2015). Finally, understanding mechanisms of injury and their longitudinal progression is paramount if we are to accurately predict recovery and develop effective therapeutics.

Diffuse axonal injury due to shearing effects in the white matter is a common diffusion MRI (dMRI)-based finding in TBI that has been associated with cognitive changes after injury. Analysis of the brain's structural connectome (SC), or the network of anatomical white matter connections obtained from dMRI, provides a window into the spatial pattern of damage that takes place when head trauma occurs. Diffusion MRI-based changes in SC have been tested as potential TBI biomarkers from many studies (Imms et al., 2019; Yuan et al., 2017), and, importantly, have been shown to be related to attention deficits (Cao et al., 2021). Additionally, analysis of the brain's functional connectome (FC), or the network representing synchrony of regional activation patterns, identified here via resting-state functional MRI (fMRI), is also informative when examining post-TBI effects. Prior research has found that TBI patients have less segregated FCs compared to non-injured controls (Imms et al., 2019) along with decreased FC integrity within the default mode network (DMN) (Mayer et al., 2011). Trauma-induced changes in both the structural and functional connectome are correlated with poor symptomatic outcomes post-injury. While the brain's FC is somewhat related to the brain's SC, it is dynamic in its ability to reconfigure to fit cognitive demands (Cohen and D'Esposito, 2016; Park and Friston,

2013; Cabral et al., 2017). For example, learning ability has been shown to depend on the dynamic flexibility of the brain's functional activity patterns (Bassett et al., 2011). The relationship between SC and FC has been shown to be related to age, sex and cognition in healthy individuals (Gu et al., 2021), and decoupling of SC and FC after TBI and in Alzheimer's disease has been related to cognitive and motor deficits (Wang et al., 2021; Sun et al., 2014; McNamee et al., 2009). Finally, remodeling of both the structural and functional connectomes after injury is associated with recovery from mild TBI; specifically an increase in a measure of the distance between SC and FC was related to better improvement in cognition from 1 to 6 months after mild TBI (Kuceyeski et al., 2019).

Though static FC analysis has provided valuable insight into mechanisms underlying TBI impairment and recovery, it fails to properly account for the dynamic nature of brain co-activation patterns, that is the synchronous activation of brain networks. The brain exhibits dynamic alternation between commonly recurring co-activation states (Karahanoglu and Van De Ville, 2015; Liu and Duyn, 2013). Cognitive control is a term that refers to the brain's ability to modify its dynamics to fit task demands (Botvinick and Cohen, 2014; Power et al., 2013; S. Gu et al., 2015). Because the brain can be modeled as a network on which this cognitive control acts, NCT is a natural model for capturing and quantifying brain dynamics. NCT is a computational approach that models the brain as an interconnected network of nodes on which activation (measured via fMRI) can flow in a directed or undirected manner. NCT allows assessment of the brain's controllability (or the ease with which the network can be driven along a given state trajectory) via assessment of transition energy (Gu et al., 2015). By mapping transition energies between states, NCT provides valuable information about the energetic landscape of brain activity in addition to biologically and cognitively relevant information about brain-state dynamics (Cornblath et al., 2020). Importantly, NCT enables the study of bidirectional information flow, meaning that asymmetry may exist in the transition energy required to go from one state to another and back again. This characteristic has been leveraged to study asymmetries in top-down versus bottom-up transitions along the cortical hierarchy (Singleton et al., 2023b; Parkes et al., 2022). Temporal dynamics and landscape energetics have been shown to be related to cognition (Karahanoglu and Van De Ville, 2015; Liu and Duyn 2013), and thus may enable better understanding of the brain's pathological changes in TBI and how it recovers (Liu and Duyn, 2013; Chen et al., 2018).

In this study, we used NCT to quantify the changing brain dynamics in individuals with mild TBI from acute to chronic stages after injury, and compared them to non-injured individuals. Individuals with mild TBI were assessed with resting-state fMRI, dMRI, and behavioral metrics at acute, subacute and chronic stages (1 week, 1 month, 6 months, and 1 year post-injury) allowing for longitudinal analysis of post-TBI changes throughout the recovery period. We additionally analyzed an independent dataset of individuals with moderate to severe TBI as a means of replicating findings and comparing and contrasting severity levels of the injury. We hypothesized that TBI would be associated with an overall steeper energetic landscape (more energy required for transitions between brain states), particularly for top-down transitions, coinciding with a shift toward increased occupancy of lower order states and decreased occupancy of higher order states. Finally, we hypothesized that these pathological shifts in transition energy and state occupancy would correlate with cognitive performance as measured by the ANT.

3. Results

We first conducted analyses on the mild TBI dataset, and the main results we present are based on this analysis; we provide a replication on the independent dataset of individuals with moderate to severe TBI. We applied k-means clustering on 135 scans from 51 TBI subjects at four different timepoints (one week, one month, six months, 12 months post-injury; not every subject was scanned at each timepoint) and 39 scans from 39 control subjects to reveal recurring states of brain activity. We

analyzed fractional occupancy of and probability of transitions between these states, comparing these metrics between control subjects and TBI subjects at each timepoint post-injury. Using NCT, we similarly analyzed state-to-state and global transition energy. Sample entropy was used to assess the complexity of global brain activity. Finally, we analyzed the relative energetic demand of top-down and bottom-up transitions post-injury and throughout the recovery window as compared to control subjects. Each of these analyses was repeated with a moderate to severe TBI dataset (42 TBI subjects over two timepoints, 17 control subjects).

3.1. Clustering of fMRI time series reveals four recurrent brain states

The four brain states shown in Fig. 1A consist of two pairs of anti-correlated states, one characterized by high and low amplitude activation in the visual network (VIS+/-) and the other by high and low amplitude activation in the default mode network (DMN+/-). High amplitude activity refers to supra-mean activation whereas low amplitude activity refers to sub-mean activation. This dichotomy is consistent with the hierarchical organization observed in previous studies (Vidaurre et al., 2017; Gutierrez-Barragan et al., 2019; Chen et al., 2018). These four states, overlapping generally with previous work, largely reflect that the task-free brain moves in a continuous way along a sensory-motor to association axis. Fig. 1B shows the similarity of the state centroid with each of the 9 functional networks. See methods for additional information on clustering and characterization of brain states.

3.2. Mild TBI causes a delayed-onset and persistent post-injury shift toward increased occupancy of lower-order states

Each individual's state time series was characterized by state

fractional occupancy (% of scan spent in each state), dwell time (how long the brain stayed in a state once transitioning to that state), and appearance rate (the number of times a state was transitioned into per minute). We found initially at 1 week post-injury that there were no differences in brain-state fractional occupancy of individuals with TBI compared to non-injured controls. However, at 1 month post-injury, a shift occurred where individuals with TBI significantly favored VIS+ and showed a trend of favoring VIS- ($t = -2.65$, uncorrected $p = 0.01$, corrected $p = 0.03$ and $t = -2.02$, uncorrected $p = 0.05$, corrected $p = 0.07$) while disfavoring DMN+ and showing a trend of disfavoring DMN- ($t = 2.60$, uncorrected $p = 0.01$, corrected $p = 0.03$ and $t = 2.04$, uncorrected $p = 0.04$, corrected $p = 0.07$) compared to controls (Fig. 2A). This deviation from the control group remained present and was statistically significant after correction for all 4 states (corrected $p < 0.05$) at 6 months post-injury. Neither dwell times nor appearance rates for the four states showed statistically significant differences across the groups.

Transition probabilities between every pair of states, along with persistence probabilities that describe the likelihood of staying in a given state, were also compared between groups (Fig. 2B). Group differences in these probabilities aligned with the observations of shifts in fractional occupancy. Again, transition probabilities at 1 week were not different from non-injured controls, but at one month post-injury there were trends of higher persistence in VIS+ ($t = -2.65$, uncorrected $p = 0.01$, corrected $p = 0.08$) and lower persistence in DMN+ ($t = 2.49$, uncorrected $p = 0.01$, corrected $p = 0.08$) for individuals with TBI. Additionally we observed trends of higher probability of transitions into both VIS states and lower probability of transitions into both DMN states for TBI patients compared to non-injured controls at all time points beyond 1 week. This effect was particularly prominent at 1 month and 6 months post-injury and less prominent at 12 months post-injury, again demonstrating a delayed and persistent alteration of post-injury

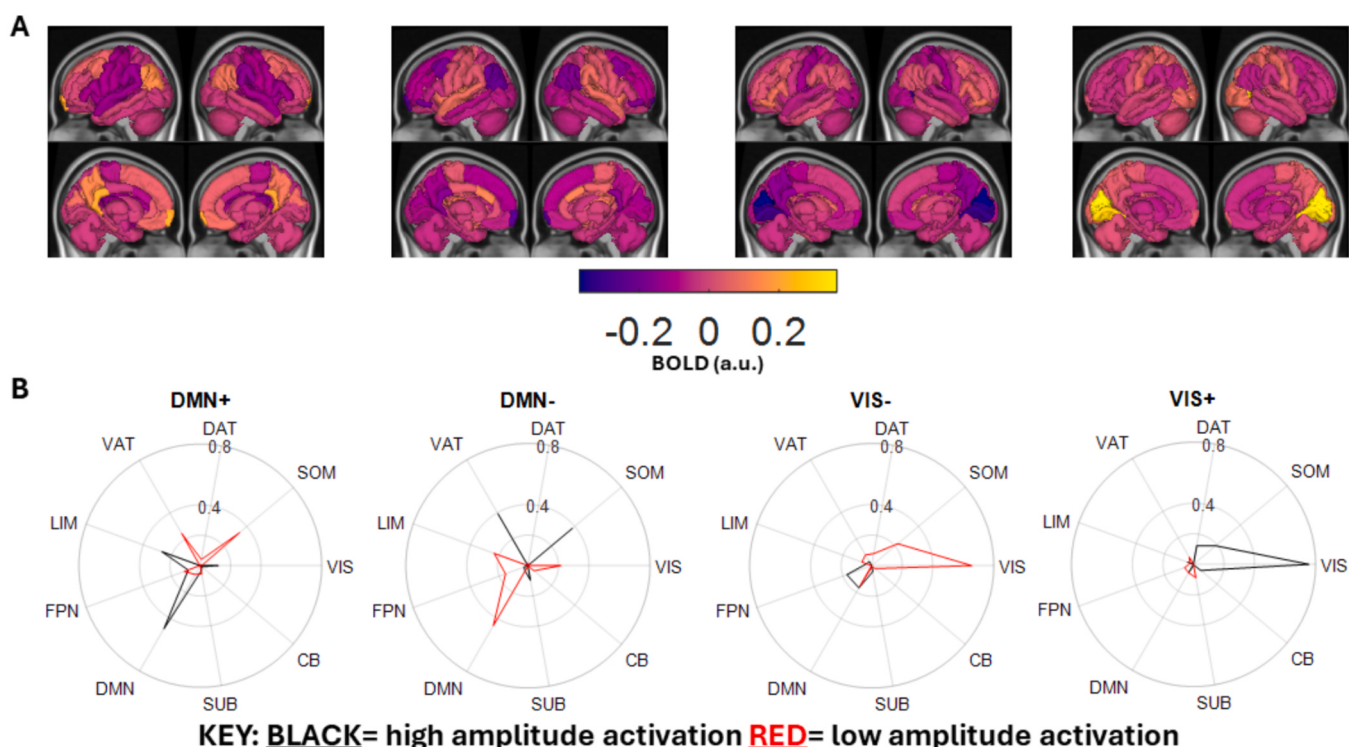


Fig. 1. Recurrent brain states. (A) The centroids of each of the four brain states, representing the average brain activity for that state. Yellow indicates high amplitude activity and purple indicates low amplitude activity. a.u. = arbitrary units B) Radial plots display the cosine similarity of each cluster centroid to the 7 Yeo functional networks, plus subcortex and cerebellum. States are labeled at the top by the most similar functional network and the type of activation (high amplitude is denoted with + and low amplitude is denoted with -). VIS = visual; SOM = somatomotor; DAT = dorsal attention; VAT = ventral attention; LIM = limbic; FPN = frontoparietal; DMN = default mode (Yeo et al., 2011); SUB; subcortex. CB = cerebellum. (For interpretation of the references to colour in this figure legend, the reader is referred to the web version of this article.)

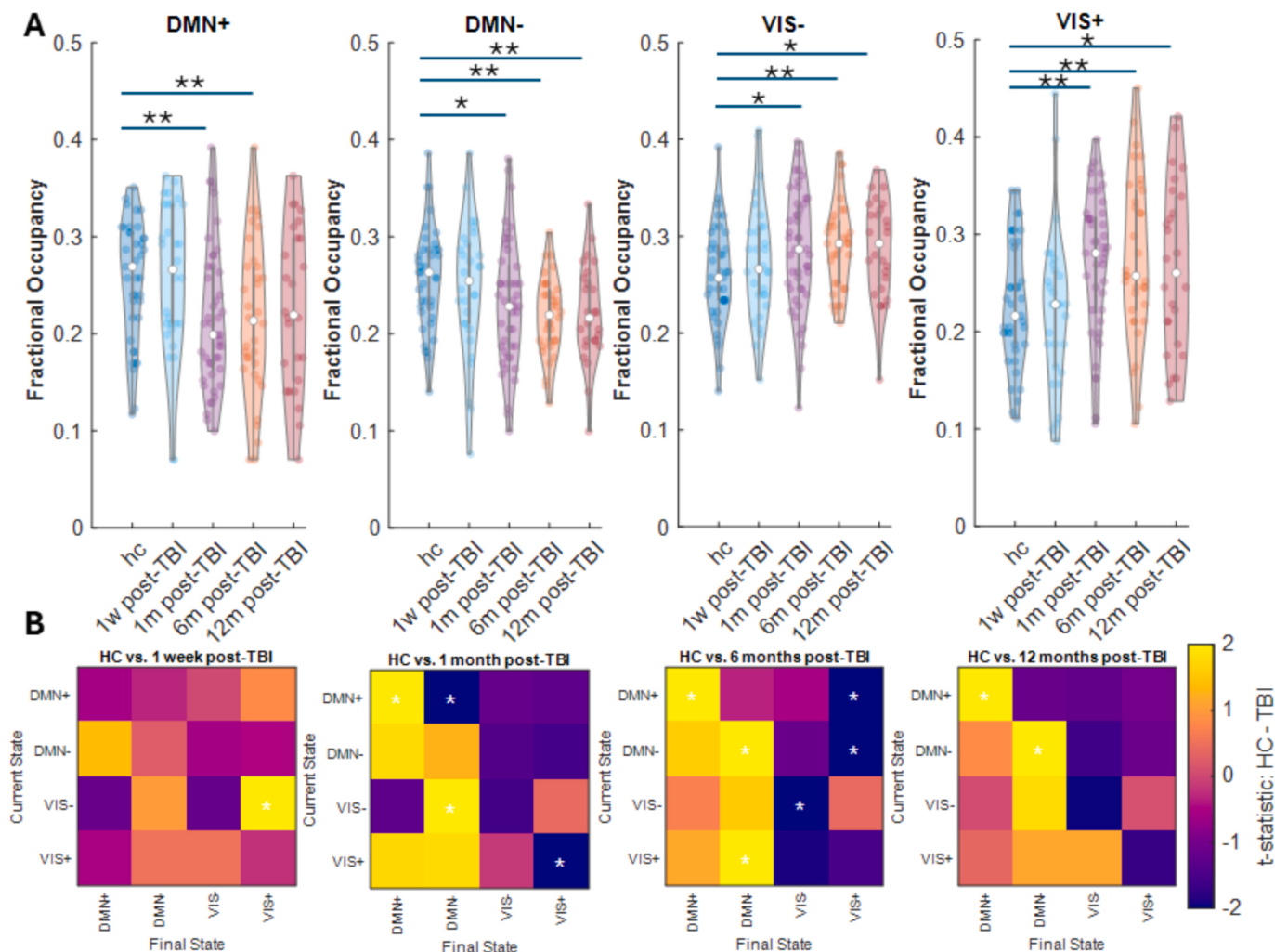


Fig. 2. Individuals with TBI show a delayed, persistent shift in brain state occupancy and dynamics, wherein they favored lower-order visual and disfavored higher-order default mode states compared to non-injured controls. (A) Fractional occupancy rates for each of the four states, for non-injured controls (hc) and individuals with TBI at each post-injury time point. (B) T-statistic of HC vs TBI groups' state-pair transition probabilities at each post-injury time point. *uncorrected $p < 0.05$ **corrected $p < 0.05$.

dynamics.

3.3. Mild TBI causes a trend of delayed decrease in global entropy and a trend of delayed increase in global transition energy that is related to worse mean reaction time

At 1 week post-injury, global transition energy (mean energy over all pairwise transitions between the four states) of mild TBI subjects was not different from that of healthy controls (HC) ($t = 0.29$, uncorrected $p = 0.78$). However, at one month post-injury we observed a trend in mild TBI subjects to higher global transition energy compared to non-injured controls ($t = -1.71$, uncorrected $p = 0.09$, corrected $p = 0.18$). This trend was also present at 12 months post-injury ($t = -1.76$, uncorrected $p = 0.08$, corrected $p = 0.18$) (Fig. 3A). We observed the inverse of this trend in global entropy, as mild TBI subjects showed a delayed trending decrease to a lower global entropy than HC at 1 month ($t = 2.25$, uncorrected $p = 0.03$, corrected $p = 0.055$) and 12 months post-injury ($t = 2.39$, uncorrected $p = 0.02$, corrected $p = 0.055$) that was not present at 1 week-post-injury (Fig. 3B). We found that mean reaction time on the ANT was negatively correlated with global transition energy (Spearman's $r = -0.31$; uncorrected $p = 0.0007$, corrected $p = 0.002$) (Fig. 3C), indicating worse performance was related to overall larger transition energies. This correlation persisted at a trend level when

considering a partial correlation between global transition energy and mean reaction time with age and sex as covariates (Spearman's $r = -0.17$, uncorrected $p = 0.08$, corrected $p = 0.08$).

3.4. Delayed transition energy increases in mild TBI show asymmetry with larger top-down vs. bottom-up increases

When investigating differences in transition energy between every pair of states (Fig. 4A), we again see a delayed-onset and persistent increase in transition energies in mild TBI compared to non-injured controls, particularly for transitions to VIS+/VIS- states. We organized the four states from higher to lower order such that the upper triangular part of the transition energy matrix represents top-down transitions and the lower triangular bottom-up transitions. If we subtract the lower from the upper triangular part of this matrix and average the result, we can obtain a measure of asymmetry in bottom-up vs top-down transition energy demand. When analyzing this asymmetry value (Fig. 4B), we see initially (1 week post-injury) no difference between mild TBI subjects and non-injured controls ($t = 0.17$, uncorrected $p = 0.86$). However, at 1 month post-injury, individuals with mild TBI show a more asymmetrical energy landscape wherein top-down transitions are more energetically demanding than bottom-up transitions ($t = 2.76$, uncorrected $p = 0.007$, corrected $p = 0.02$), a difference that was also significant at 12

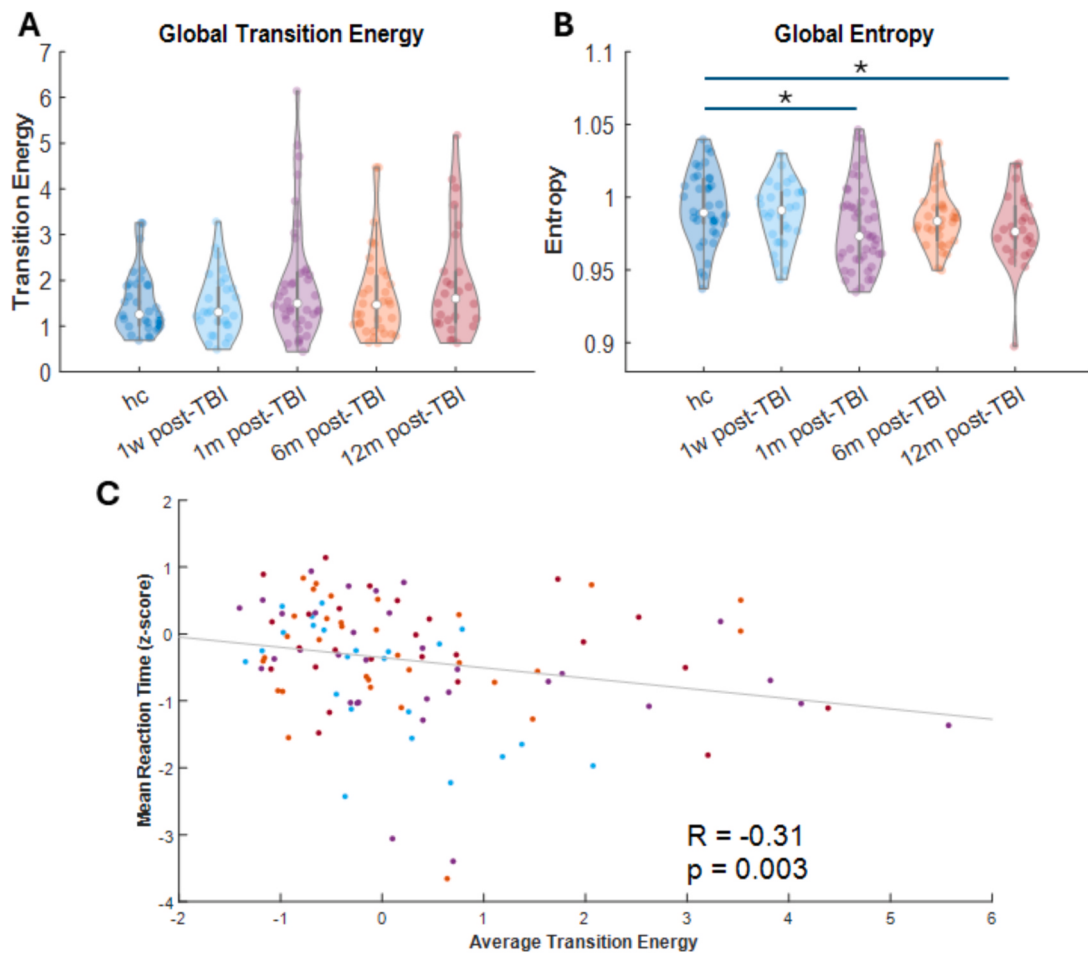


Fig. 3. Individuals with mild TBI show a trend toward delayed increase in global transition energy (and a significant decrease in global entropy) in such a way that is correlated with mean reaction time. (A) Global transition energy for non-injured controls and individuals with mild TBI at each time point. (B) Global entropy for non-injured controls and individuals with TBI at each time point. (C) Spearman correlation between global transition energy and MRT for individuals with mild TBI at each timepoint. Points are colored by their collection time post-injury. p-value displayed is corrected. *uncorrected $p < 0.05$.

months post-injury ($t = 2.60$, uncorrected $p = 0.01$, corrected $p = 0.02$).

3.5. Replication using $k = 6$ states

We re-ran our analyses of the mild TBI data with 6 states (instead of 4) and found largely similar results. In short, there was a delayed-onset and persistent trend toward increased (some significant) fractional occupancy of the VIS+/- state and decreased occupancy of the other 4 states that had more contributions from the DMN. We found a trend-level increase in the ratio of top-down transition energy to bottom-up transition energy in mild TBI at 3 months and 12 months post-injury compared to non-injured controls. We also found a trend of increased energy for transitions into VIS- states (and at 12 months also VIS + state transitions). Finally, we saw a trend toward global transition energy being negatively correlated with mean reaction time. The details of this replication analysis can be found in the SI.

3.6. Linear mixed effect modeling

We completed additional investigation of the relationships between transition energy, entropy and MRT via an LME model. This failed to show any significant effect between transition energy and entropy as explanatory variables and MRT as a response variable. Model information and statistics are given in the SI.

3.7. Replication using an independent, moderate to severe TBI dataset

We re-ran all of the above analyses on an independent set of imaging and attention measures collected from 42 individuals with moderate to severe TBI at two scan time points: 4–6 months post-injury and 12 months post-injury. Single scans from each of 17 non-injured controls were also compared.

An optimal of 4 states was found in the moderate to severe TBI dataset, and overall the centroids showed coactivation of a higher number of networks (SI Fig. 6) compared to the mild TBI states which were largely each dominated by activation of a singular network (Fig. 1). Moderate to severe TBI subjects did not significantly differ from HC in fractional occupancy of the 4 states, but the TBI subjects had non-significantly lower occupancy of the DMN + state (SI Fig. 7A). A trend of increase ($t = -2.46$; uncorrected $p = 0.03$, corrected $p = 0.22$) was observed in dwell time of the state dominated by low amplitude activation of the subcortical network (SUB-, the state which also had the second highest VIS activity of the four states) at 4–6 months post-injury compared to HC (SI Fig. 7C), and this was mirrored by a trend-level increase in persistence probability for SUB- at both 4–6 months ($t = -2.49$; uncorrected $p = 0.02$, corrected $p = 0.13$) and 12 months post-injury ($t = -2.20$; uncorrected $p = 0.04$, corrected $p = 0.13$) compared to HC (SI Fig. 7B). A trend-level decrease ($t = 2.53$; uncorrected $p = 0.01$, corrected $p = 0.13$) was observed in transition probability from SUB- to VIS + in moderate to severe TBI subjects 4–6 months post-injury compared to HC (SI Fig. 7B).

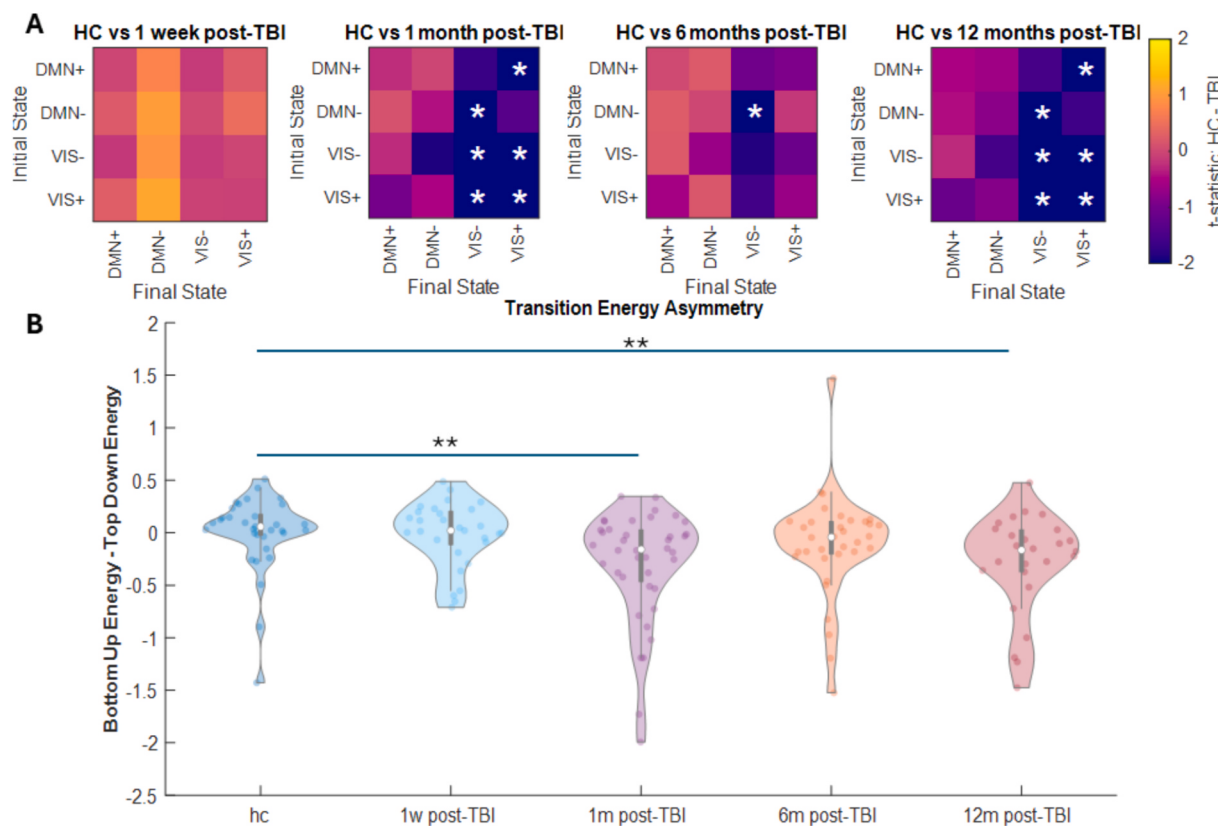


Fig. 4. Individuals with TBI have decreased bottom-up versus top-down transition energy asymmetry. (A) T-statistics of the group differences (HC vs. individuals with mild TBI) in transition energies between pairs of brain states at each time point. (B) Transition energy asymmetry (the average difference between bottom up transition energy minus top down transition energy) for each pair of states *uncorrected $p < 0.05$ **corrected $p < 0.05$.

Moderate to severe TBI subjects at 4–6 months post-injury did not show a significant difference from HC in global transition energy but showed a delayed shift at 12 months post-injury to a significantly increased global transition energy relative to HC ($t = -2.47$, uncorrected $p = 0.02$, corrected $p = 0.04$) (Fig. 5A). Global entropy of moderate to severe TBI subjects was not significantly different from that of HC (Fig. 5B), but the directionality observed was the same as in the mild TBI subjects ($t = 1.40$, uncorrected $p = 0.18$ at 12 months post-injury). The difference between bottom-up and top-down transition energy did not show change in moderate to severe TBI subjects compared to HC (Fig. 5C). The correlation between global transition energy and mean reaction time for moderate to severe TBI subjects was positive (Fig. 5D) both within the raw correlation (Spearman's $r = 0.25$, uncorrected $p = 0.06$, corrected $p = 0.06$) and for the partial correlation with age and sex as covariates (Spearman's $r = 0.27$, uncorrected $p = 0.05$, corrected $p = 0.06$). The delayed increase in transition energy of moderate to severe TBI subjects was not as transition-specific as it was for mild TBI (Fig. 5E).

4. Discussion

Here we use NCT to quantify the effect of mild and moderate to severe TBI on the brain's dynamics landscape from acute to chronic post-injury stages. Most prominently, our results support the idea of a delayed shift in the dynamics of the brain in response to injury. In mild TBI, our analysis of fractional occupancy showed a shift at one month post-injury to increased occupancy of lower order visual dominant states and decreased occupancy of higher order default mode network dominated states. On the same time scale, we observed an increase in the energy requirement particularly for transitions into visual dominant states. Coinciding with these changes, we noted that the energy requirement for top-down transitions showed an increase relative to that

of bottom-up transitions at one month post-injury. In addition to the evidence of a transition-specific delayed increase in transition energy, we found a delayed decrease in global entropy also at one month post-injury. We demonstrate the cognitive relevance of the energetic shift through the correlation between transition energy and mean reaction time on the ANT. Furthermore, we show the robustness of this finding through our analysis of independent moderate to severe TBI data which also displayed a delayed steepening of the energy landscape. The observed shifting dynamics supports the idea that functional reorganization and structural damage following head trauma occurs over a period of continuous alteration in the months to years following injury and may be relevant to recovery.

We observed that transition energy increased predominantly for transitions into the VIS + and VIS- states (Fig. 4A). In our version of the transition energy calculations, energy depends on brain activity patterns as well as the strength of the white matter structural connections (Gu et al., 2015). Decreased structural connectivity (which occurs after TBI) would thus most likely result in increased energy as the diffusion process on which this metric depends would be slower. In moderate and severe TBI, Chiou et al. reported dynamic white matter change taking place beyond the initial recovery phase, as fractional anisotropy of the frontal and temporal regions showed an initial decrease followed by an ongoing increase in the 3 years following (Chiou et al., 2019). Meningher et al. noted a similar trend in mice, where global efficiency of the right hemisphere increased in the first week post-injury but decreased thereafter (Meningher et al., 2020). Our finding reflecting delayed-onset increases in transition energy additionally may relate to the concept of secondary structural connectivity damage described in prior publications on the mechanism of TBI (Ng and Lee 2019) where longer term effects such as excitotoxicity (van Landeghem et al., 2006; Chamoun et al., 2010), neuroinflammation (Gentleman et al., 2004; Lotocki et al.,

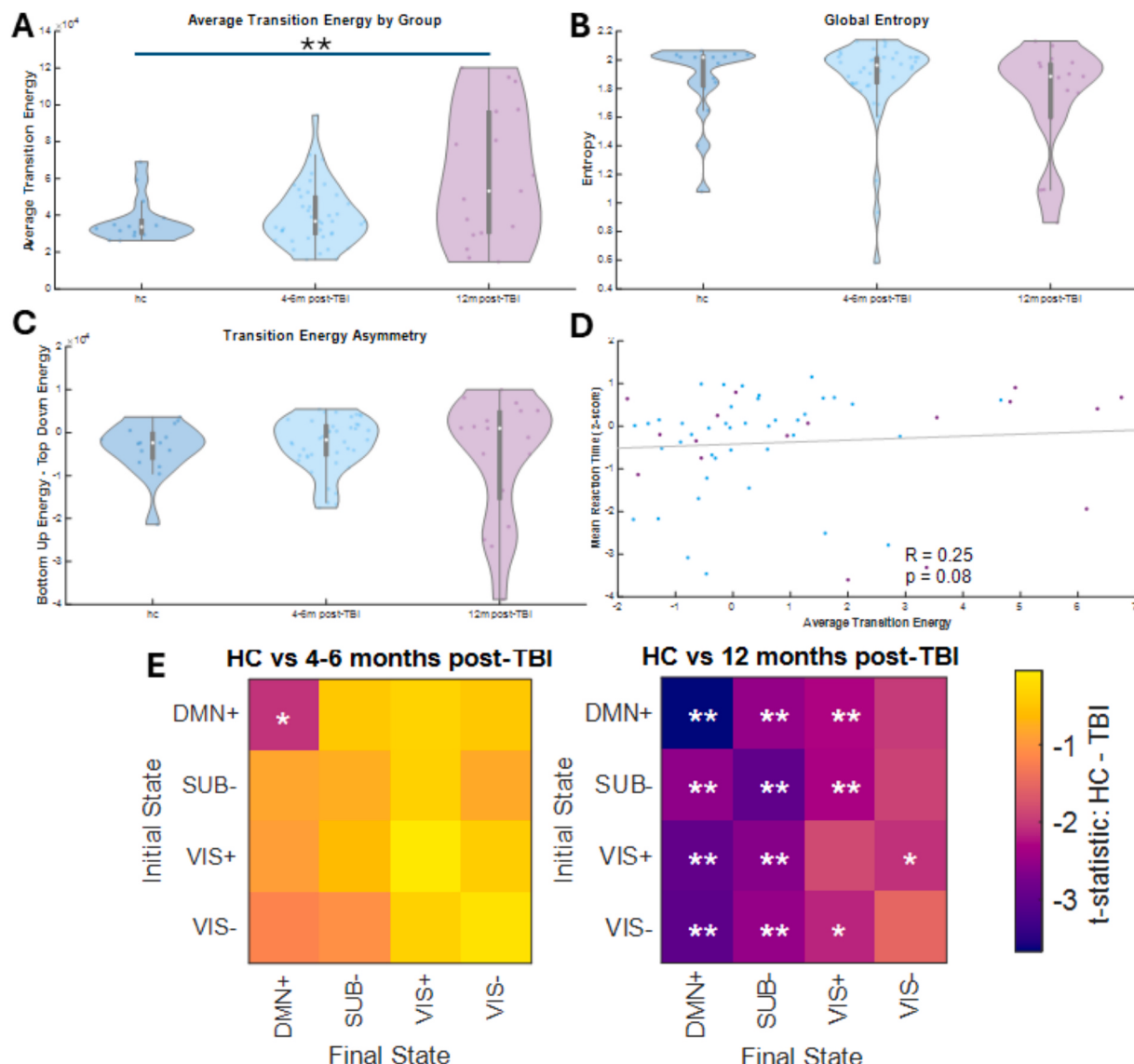


Fig. 5. Independent, moderate to severe TBI dataset shows delayed global transition energy increase and correlation between energy and attention. (A) Global transition energy for HC and TBI patients at each time point. (B) Global entropy for HC and TBI patients at each time point. (C) Transition energy asymmetry by group given by the average difference between bottom up transition energy and top down transition energy for each set of pairwise transitions. (D) Spearman correlation between global transition energy and MRT for TBI patients at each timepoint. p-value displayed is corrected. (E) T-statistics of the group differences in transition energies between brain activity states in HC vs. TBI subjects at each time point *uncorrected $p < 0.05$ **corrected $p < 0.05$.

2009; Johnson et al., 2013), mitochondrial dysfunction (Xiong et al. 1997), and axon degeneration (Povlishock 1992; Büki and Povlishock 2006) have been implicated in delayed-onset injury-related damage.

The brain's functional response to this structurally-defined change is notable in that significantly increased occupancy of VIS+ and VIS- and significantly decreased occupancy of DMN+ and DMN- coincide with the significant increase in transition energy required to move into the VIS states (Fig. 2, Fig. 4). The shift in occupancy is consistent with prior work showing increased functional connectivity of the visual network and reduced functional connectivity of the DMN in semi-acute mild TBI (Palacios et al., 2017). Our recent work demonstrated a link between fractional occupancy of states and functional connectivity (Olafson et al., 2022). Specifically, higher occupancy of states characterized by co-activation of two regions/networks results in a stronger FC between those two regions/networks. The default mode network has been previously shown to be one of the most globally connected regions in the brain (Cole, Pathak, and Schneider 2010), and connectivity here has been demonstrated to be cognitively relevant (Shafer et al., 2021).

Reduced structural and functional connectivity of the DMN have been associated with cognitive decline as part of regular aging in addition to pathology (Damoiseaux et al., 2008; Spreng and Turner 2013; Tomasi and Volkow 2012; Buckner et al., 2009; Moretto et al., 2022; Varangis et al., 2019; Zonneveld et al., 2019). The *integrity hypothesis of default network function* asserts that hypoactivation and hypoconnectivity of the DMN negatively impact self-generated cognitive action (Andrews-Hanna et al., 2014).

The observed shift in VIS occupancy may also relate to clinically-observable TBI symptoms. Primary vision deficits are commonly noted in TBI as are symptoms related to the integration of vestibular and visual input (Armstrong 2018; Hac and Gold 2022; Padula et al., 2017). Abnormalities and long-term motor sequelae of eye-tracking, posture, photophobia, and balance are of concern (McNamee et al., 2009; Dever et al., 2022). Future work will associate occupancy of the VIS states with visual symptom severity.

In NCT, controllability can be defined as the ease at which a network can be driven along a given state trajectory and is inversely proportional

to input energy. We utilize network controllability for information on the cognitive control, or task-adaptability provided by given brain dynamics. Gu et al. noted that the DMN is a region of high average controllability and postulated that this demonstrates its role as a control point for the rest of the brain (Gu et al., 2015). Moreover, they describe the DMN as a ground state activated at rest that can transition the brain into task-based “excited” states where other networks (including VIS) are activated (Gu et al., 2015). In these terms, our results can be interpreted to say that mild TBI diminishes the controllability of the brain by prompting an increased reliance on high energy excited states.

Energetic analyses of the brain may be relevant for considering cognitive deficits following injury. We observed that global transition energy was significantly negatively correlated with cognitive performance on the MRT task of the ANT (Fig. 3C). This trend supports the idea that, on a macroscopic level, higher energy requirements relate to poor cognitive performance. This follows on the idea from NCT that an input of transition energy for a given trajectory among state space is related to the effort required for such action (Gu et al., 2015). Our energetic analyses of TBI then support the idea that cognitive inefficiencies are created by an increase in the energetic demand and thus effort requirement for regular everyday functioning.

The increased energetic demand observed in the mild TBI patients studied here was found to be larger in top-down transitions (Fig. 4B). Top-down processing streams are associated with goal-driven tasks such as those measured with the ANT’s MRT metric. Furthermore, inefficiencies in top down processing may be responsible for cognitive deficits previously noted in TBI, namely within the category of executive functioning. Top-down processing is crucial for emotion regulation, and a heightened energetic barrier for such processing may relate to the emotional disturbances and coping difficulties previously noted in TBI (J et al., 2015; Wang et al., 2022; Gorgoraptis et al., 2019). The top-down energy increase may also relate to more serious neuropsychiatric sequelae which have been noted following TBI (Howlett et al., 2022). Particularly, the rise in top-down transition energy may offer explanation for the development and/or exacerbation of mania-like poor impulse control which has been noted in the time following head trauma (Rao and Lyketsos, 2000). Alterations in top-down connections have also been pinpointed in previous work as a neural correlate with self-injurious behaviors (Auerbach et al., 2021). As this topic is explored further, it is probable that the association between energetic demand and TBI-related cognitive disruptions can be defined even further in terms of the mechanistic link.

Our analysis of moderate to severe TBI (Fig. 5) largely replicates the trends observed among the mild TBI subjects and may also serve as a starting point for future research on the differences between mild, moderate, and severe TBI. Notably, we again found evidence of a delayed increase in the energy requirement for transitions into visual dominant states, though it was first noted at 12 months post-injury whereas the same was noted in mild TBI at 1 month post-injury. It is important to note that the first scans were obtained from the moderate to severe TBI patients at 4–6 months post-injury, so neuroimaging data from the acute phase may provide further information on how this injury’s longitudinal progression compares to that of mild TBI. Though entropy of moderate to severe TBI subjects didn’t show a significant difference from control subjects, the overall trend was a decrease in this metric between 4–6 months and 12 months post-injury, again aligning to the findings in the mild TBI dataset. Interestingly, moderate to severe TBI subjects showed a positive correlation between global transition energy and MRT on the ANT, opposing the observation of a negative correlation in the mild TBI data. It is possible that this is related to increased functional compensation mechanisms reflecting the higher level of trauma experienced in this group. We did not observe a significant shift in occupancy in tandem with the energy shift of moderate to severe TBI as we did in mild TBI (SI Fig. 7A and 9A) but we did see a non-significant decrease in DMN state occupancy and an increase in dwell time of a state with the second-highest VIS activity. It is possible that

severity of trauma may moderate the relationship between dynamics and energetics, but it is also important to consider that these are two independent datasets with differences present in demographics, injury severity and MRI collection and processing.

5. Limitations and future work

Though the addition of the moderate to severe TBI dataset is valuable and informative in verifying the general trends observed in mild TBI, the differences between the datasets in patient makeup and post-injury intervals make explicit comparison of the results challenging. Additionally, although these two datasets utilized different data acquisition and preprocessing protocols, these differences are minimized by comparing within-subject longitudinal trends within each dataset. It may be beneficial to run further analyses on larger mild and moderate to severe TBI subjects using identical data collection patterns to assess the effect of injury severity on brain dynamics across the severity spectrum.

Though this study used data from 51 mild TBI subjects and there were 4 data collection timepoints following injury, only 135 total TBI data points were collected, meaning that not every subject had data collected at each time point. Likewise, only 17 out of the 42 moderate to severe TBI subjects had follow-up data. This presents a greater degree of uncertainty in making generalizations regarding longitudinal trends in TBI recovery. It also is worth noting here that no distortion correction was applied to the DWI data as no fieldmap data was available for this study. Follow-up work may benefit from sourcing data from a protocol where this correction can be applied.

In this work, we uncover several meaningful relationships between structure, function, and cognition. However, we must acknowledge the fact that the linear mixed effect modeling (see SI) fails to show significance in relating cognition to brain dynamics. With this, it is important to consider that changes in the brain throughout recovery may be inherently non-linear or non-stationary over time.

Finally, it is worth emphasizing that the transition energy in our analyses should be interpreted as the magnitude of the input that the structural connectome requires in order to obtain a desired state transition (Gu et al., 2015; Singleton et al., 2022). Our energy analysis is not the metabolic energy that is commonly considered in biological contexts, although recent work has suggested they may be related (He et al., 2022).

6. Conclusion

Using principles of NCT, we jointly analyzed structural and functional imaging along with ANT to model the brain’s changes following mild and moderate to severe TBI. We present evidence for a delayed response mechanism where brain changes in dynamics are most prominent in the month following injury and persist somewhat at 12 months after injury. This delayed shift in dynamics includes a significant increase in transition energy to move between brain states, particularly for top-down transitions. Additionally, we show that the brain begins to prefer occupancy of bottom-up states (VIS+/VIS-) as opposed to top-down states (DMN+/DMN-) when this delayed shift in dynamics occurs. We combine these analyses with attention task performance and show an association between the increase in transition energy and worse attention performance. This work demonstrates that NCT is a useful tool with which we can study the evolution of brain dynamics after injury. Understanding post-injury longitudinal trajectories of brain dynamics is crucial if we aim to design therapies that may support recovery.

7. Methods

7.1. Cohort characteristics, data acquisition and MRI preprocessing (Mild TBI)

Neuropsychological test scores and MRI data were collected from 51

subjects (29.6 ± 8.6 years of age, 35 males) that incurred mild TBI. Data was collected at 1 week, 1 month, 6 months, and 12 months post-injury. 8 of the mild TBI subjects had complete datasets with measurements at all 4 timepoints, and the others were analyzed for between 1 and 3 timepoints. Mild TBI was defined as having Glasgow Coma Scale of 13–15 at injury, loss of consciousness less than 30 min, and post-traumatic amnesia less than 24 hrs. MRI data was collected from 39 HC subjects for comparison, but these subjects did not undergo neuropsychological tests. A 3 T GE Sigma EXCITE scanner with an eight channel phased array head coil was used to collect the MRI data which included structural scans (FSPGR T1, $1 \times 1 \times 1 \text{ mm}^3$ voxels), eyes-closed resting state fMRI (7 min, $3.4 \times 3.4 \times 4.0 \text{ mm}^3$, TR/TE = 2000/28 ms), and 55-direction high angular resolution dMRI ($b = 1000 \text{ s/mm}^2$, 7 volumes with $b = 0, 1.8 \times 1.8 \times 1.8 \text{ mm}^3$ voxels, TR/TE = 14000/63 ms). Neuropsychological metrics consisted of nine ANTsubscores and sixteen California Verbal Learning Test-II (CVLT-II) subscores (Fan et al., 2002; Jacobs and Donders, 2007). These tests were based on recall and recognition ability and were used as measures of cognitive performance to be analyzed throughout recovery.

Gray and white matter tissue were separately grouped and gray matter was further separated into 86 automated regions of interest using the semiautomated FreeSurfer software (Fischl, 2012). Cortical and subcortical parcellations were used in the construction of the functional and structural connectivity network, with details outlined in our previous publication (Kuceyeski et al., 2019). In short, fMRI was processed using the CONN toolbox (Nieto-Castanon and Whitfield-Gabrieli, 2021) to perform motion correction (simultaneous realignment and unwarping, via non-linear registration to anatomical scan), slice-timing correction, coregistration/normalization to 3 mm MNI space, followed by outlier removal. Regional time series were averages of the voxel-wise time series. Diffusion MRIs were linearly motion corrected using a modified version of FSL's eddy_correct and the linear correction applied to the gradient directions. The dMRIs were then corrected for eddy currents using FSL's eddy_correct. Orientation distribution functions were constructed using FSL's BEDPOSTX (two fiber orientations), gray/white matter masks linearly transformed to dMRI space and streamline tractography performed from each voxel in the gray matter/white matter interface. Pairwise region of interest (ROI) streamline matrices were extracted and normalized by the total volume of each pair of ROIs.

Subject retention across time

Timepoint	1	2	3	4
1	X	27/30	19/30	14/30
2	27/45	X	34/45	25/45
3	19/34	34/34	X	21/34
4	14/26	25/26	21/26	X

*12 subjects had scans at all 4 timepoints.

In table, row 1 tells how many of the subjects from timepoint 1 also had scans taken at each of the other timepoints (denominator is the same across each row). Row 2 tells how many of the subjects with scans at timepoint 2 also had scan taken at each of the other timepoints, etc., etc.

**11 fMRI scans did not have diffusion MRI: 6T2, 4 HC, 1T1.

7.2. Cohort characteristics, data acquisition and MRI preprocessing (moderate to severe TBI)

Neuropsychological test scores and MRI data were collected from 42 subjects that incurred TBI. Data was collected at 6 months and 12 months post-injury. 17 of the TBI subjects had complete datasets with measurements at both timepoints, and the others were analyzed only at 6 months post-injury. TBI subjects in this cohort were required to have sustained a complicated mild (Glasgow Coma Scale score of 13–15 with evidence of intracranial lesion as verified on acute neuroimaging) or moderate-severe TBI (Glasgow Coma Scale score ≤ 12) within the last 6

months. MRI data was collected from 15 HC subjects for comparison.

All participants were required to meet the following criteria: (i) 18 years of age or above; (ii) English-speaking; (iii) capable of providing informed consent or a proxy/authorized agent available to provide informed consent; (iv) physically healthy and able to safely undergo PET imaging; (v) not currently taking any psychoactive or benzodiazepine drugs; (vi) not currently taking any medication for attention-deficit/hyperactivity disorder; (vii) no history of schizophrenia, drug, or alcohol abuse; (viii) no history of epilepsy, stroke, dementia, or serious medical illness by self-report; and (iv) not pregnant (for female participants).

MRI data was collected on a 3T Siemens Prisma scanner with a 32-channel head coil, using a protocol based on the HCP Lifespan study (Harms et al., 2018). Data include 0.8 mm isotropic T1w and T2w anatomical scans, 11 min of eyes-open rsfMRI divided into two scans with opposing A>P and P>A phase-encoding (2 mm isotropic, TR/TE = 800/37 ms, multi-band factor 8, 420 volumes per scan), and multi-shell diffusion data (1.5 mm isotropic, TR/TE = 3230/39.2 ms, multi-band factor 4, 92 directions/shell at $b = 1500/3000$, $b = 0$ every 16 volumes, acquired in both A>P and P>A). A matching pair of spin echo field maps with opposing phase encoding direction was collected for each resting state scan.

MRI data was preprocessed using the HCP minimal processing pipeline (Glasser et al., 2013). Preprocessed fMRI was further processed using custom scripts to identify and exclude outlier timepoints (motion derivative threshold 0.9 mm, global signal threshold 5σ) and nuisance regressors related to motion and CSF and white-matter signals (24 motion time series (Power et al., 2014) and 10 eigenvectors derived from eroded white matter and CSF masks (Behzadi et al., 2007)), temporally filter the final result (high-pass filter cutoff 0.008 Hz, using DCT projection), and to extract average ROI time series. Outlier timepoints were excluded from nuisance regression and temporal filtering. For diffusion data, MRtrix3 was used to perform bias correction, constrained spherical deconvolution, and whole-brain deterministic tractography (Tournier et al., 2012). Pairwise ROI streamline matrices were extracted and normalized by the total volume of each pair of ROIs.

7.3. Brain states

Brain states were extracted, characterized, and analyzed as in Cornblath et al. (Cornblath et al., 2020). All subjects' fMRI time series (control and TBI together) were concatenated in time, producing a 29,754 X 86 matrix ((TR x scans)X ROI), and k-means clustering was used to identify recurrent activation patterns, or brain states. Following clustering, brain states were z-scored across regions, resulting in vectors containing both positive and negative values that reflect relative activation magnitudes. This treatment of brain states is consistent with standard practices in prior NCT applications (Cornblath et al., 2020). Using Pearson correlation as a distance metric, the clustering solution with the best separation of data was chosen among 50 repetitions. For further assessment of stability and reliability of the clustering solution, this process was independently repeated 10 times, and the adjusted mutual information (AMI) was compared between each of the 10 partitions. The partition with the greatest total AMI with the other nine partitions was selected for analysis. We plotted the variance explained for the range of $k = 2$ clusters to $k = 14$ clusters and observed an “elbow” in the plot at $k = 4$ –6 (Fig. S1). After $k = 6$, the amount of variance explained by adding an additional cluster was negligible. We report the results for $k = 4$ in the main text and the results for $k = 6$ in the supplement.

7.4. Characterization of brain states

The centroid of each of the four clusters was characterized based on cosine similarity to the seven resting state networks (RSNs) presented by Yeo et al (Yeo et al., 2011). Considering that the mean signal was

removed from each scan's regional time series, positive values in the centroid reflect high amplitude activation (above the mean) while negative values in the centroid reflect low amplitude activation (below the mean). We calculated the Spearman correlation values between all centroids to quantify the relationship between them.

7.5. Temporal dynamics

The temporal dynamics of the earlier determined brain states were used to describe changes induced by TBI. For each state, the fractional occupancy was determined by the number of TRs (repetition times) assigned to the cluster divided by the total number of TRs. Dwell time was calculated as the mean amount of time spent per visit to each state. Appearance rate was calculated by finding the average amount of times each state was transitioned into per minute. Transition probabilities were also obtained for each state to state transition by calculating the probability that any given state i was followed by state j . Unpaired t-tests for differences between means were performed to assess group differences in these metrics between the five groups (controls and four TBI timepoints).

7.6. Ranking brain states: top-down vs. bottom-up

The dot product was taken of the absolute value of each centroid vector with a functional connectivity gradient vector indicating each of the 86 regions' positions in the top-down vs. bottom-up processing hierarchy (Margulies et al., 2016). This allowed the centroids to be ranked in order of most top-down to least top-down (bottom-up). This ranking was then utilized to compare transition energies for top-down vs bottom-up transitions.

7.7. Transition energy calculations

We utilized individual-level brain states from each scan to quantify state transition energies using NCT. Transition energy here is defined as the minimum energy input into a network—here, the structural connectome— required to move from one state to another (Karrer et al., 2020). We modeled neural dynamics using a linear, time-invariant model:

$$\frac{dx}{dt} = Ax(t) + Bu(t), \quad (1)$$

where A is an individual's NxN structural connectivity matrix (normalized by its maximum eigenvalue plus 1 and subtracted by the identity matrix to create a continuous system) (Karrer et al., 2020), $x(t)$ is the regional activation at time t , B is the NxN matrix of control points, and $u(t)$ is the external input into the system. Here, N is the number of regions in our parcellation, i.e. 86. We selected $T = 1$ for the time-horizon and the identity matrix for B , as in previous studies (Karrer et al., 2020; Tozlu et al., 2023; Singleton et al., 2022; Singleton et al., 2023b; Luppi et al., 2023; Parkes et al., 2022; 2023; Singleton et al., 2023a). Integrating $u(t)$ over the time-horizon for a given transition yields the total amount of input that was injected into each region to complete the transition between states, and summing that value over all regions then gives the total amount of energy necessary to be injected over the whole brain. This summation represents *transition energy*. We calculated the pairwise transition energies between each of the four brain-states for each individual using this framework. In cases where the initial and target state were the same (Fig. 4, diagonal), transition energy was the energy required to maintain that state (i.e. resist the natural diffusion of activity through the SC). Average transition energy for each individual was calculated as the mean over all transitions. Transition energies were compared for top down transitions vs. bottom-up transitions using the ordering method previously described. Unpaired t tests for differences between means were again performed to assess group

differences in these metrics between the five groups (controls and four TBI timepoints). Spearman correlations were calculated for the relationship between transition energy into a given state and fractional occupancy of that same state.

7.8. Entropy calculations

Sample entropy is defined as the negative logarithm of the conditional probability that two similar sequences of m points in a time-series remain similar at the next point $m + 1$, counting over all other vectors except itself (Delgado-Bonal and Marshak 2019). Two sequences are considered similar if they have a Euclidean distance less than r . Here we used $m = 3$ and $r = 0.2\sigma$, where σ is the standard deviation of the time-series, based on prior work (Tozlu et al., 2023; Tomčala 2020; Z. Wang et al., 2014). Sample entropy was calculated for each of the 86 regional time-series of each subject and the global entropy was the average of these values. This process was repeated for each timepoint, allowing for longitudinal entropy analysis via unpaired t-tests. Spearman correlations were calculated for the relationship between entropy and transition energy.

7.9. Correlations with cognition

ANT MRT values were adjusted for age and standardized such that numbers greater than 0 indicate a faster reaction time than average healthy controls and numbers below 0 indicate a slower reaction time than average healthy controls. Spearman correlations were calculated between global transition energy and MRT using TBI patient data only.

7.10. Multiple comparisons

P-values were corrected for multiple comparisons using the Benjamini-Hochberg method (Benjamini and Hochberg, 1995) where indicated.

7.11. Code availability

Code for clustering time-series, analyzing brain-state dynamics, and calculating transition energy are available at https://github.com/ejcorn/brain_states. Code for other statistical analyses and figures can be made available upon request.

CRediT authorship contribution statement

Nate Roy: Writing – review & editing, Writing – original draft, Investigation, Formal analysis, Conceptualization. **S. Parker Singleton:** Writing – review & editing, Supervision, Methodology, Formal analysis, Conceptualization. **Keith Jamison:** Writing – review & editing, Methodology, Data curation. **Pratik Mukherjee:** Funding acquisition, Data curation. **Sudhin A. Shah:** Writing – review & editing, Funding acquisition, Data curation. **Amy Kuceyeski:** Writing – review & editing, Supervision, Resources, Methodology, Funding acquisition, Conceptualization.

Funding Information

This work was supported by the following NIH grants: R01 NS060776 [P.M.], R01 NS102646-01A1 [A.K. and S.S.], and RF1 MH123232 [A.K.]. P.M. has received research support from GE Healthcare and serves on the Medical Advisory Board of the GE-NFL Head Health Initiative.

Declaration of Competing Interest

The authors declare that they have no known competing financial interests or personal relationships that could have appeared to influence

the work reported in this paper.

Appendix A. Supplementary data

Supplementary data to this article can be found online at <https://doi.org/10.1016/j.nicl.2025.103799>.

Data availability

Data will be made available on request.

References

- Andrews-Hanna, J.R., Smallwood, J., Nathan Spreng, R., 2014. The default network and self-generated thought: component processes, dynamic control, and clinical relevance. *Ann. N. Y. Acad. Sci.* 1316 (1), 29–52. <https://doi.org/10.1111/nyas.12360>.
- Armstrong, R.A., 2018. Visual problems associated with traumatic brain injury. *Clin. Exp. Optom.* 101 (6), 716–726. <https://doi.org/10.1111/cxo.12670>.
- Auerbach, R.P., Pagliaccio, D., Allison, G.O., Alqueza, K.L., Alonso, M.F., 2021. Neural correlates associated with suicide and non-suicidal self-injury in youth. *Biol. Psychiatry* 89 (2), 119–133. <https://doi.org/10.1016/j.biopsych.2020.06.002>.
- Bassett, D.S., Wyombs, N.F., Porter, M.A., Mucha, P.J., Carlson, J.M., Grafton, S.T., 2011. Dynamic reconfiguration of human brain networks during learning. *PNAS* 108 (18), 7641–7766. <https://doi.org/10.1073/pnas.1018985108>.
- Behzadi, Y., Restom, K., Liu, J., Liu, T.T., 2007. A component based noise correction method (CompCor) for BOLD and perfusion based fMRI. *Neuroimage* 37 (1), 90–101. <https://doi.org/10.1016/j.neuroimage.2007.04.042>.
- Benjamini, Y., Hochberg, Y., 1995. Controlling the false discovery rate: a practical and powerful approach to multiple testing. *J. Roy. Stat. Soc.: Ser. B (Methodol.)* 57 (1), 289–300.
- Botvinick, M.M., Cohen, J.D., 2014. The computational and neural basis of cognitive control: charted territory and new frontiers. *Cognit. Sci.* 38 (6), 1249–1285. <https://doi.org/10.1111/cogs.12126>.
- Buckner, R.L., Sepulcre, J., Talukdar, T., Krienen, F.M., Liu, H., Hedden, T., Andrews-Hanna, J.R., Sperling, R.A., Johnson, K.A., 2009. Cortical hubs revealed by intrinsic functional connectivity: mapping, assessment of stability, and relation to Alzheimer's disease. *J. Neurosci.* 29 (6), 1860–1873. <https://doi.org/10.1523/JNEUROSCI.5062-08.2009>.
- Büki, A., Povlishock, J.T., 2006. "All Roads Lead to Disconnection?—Traumatic Axonal Injury Revisited." *Acta Neurochirurgica* 148 (2): 181–93; discussion 193–194. <https://doi.org/10.1007/s00701-005-0674-4>.
- Cabral, J., Kringselbach, M.L., Deco, G., 2017. Functional connectivity dynamically evolves on multiple time-scales over a static structural connectome: models and mechanisms. *Neuroimage* 160 (October), 84–96. <https://doi.org/10.1016/j.neuroimage.2017.03.045>.
- Cao, M., Luo, Y., Ziyang, Wu, Mazzola, C.A., Catania, L., Alvarez, T.L., Halperin, J.M., Biswal, B., Li, X., 2021. Topological aberrance of structural brain network provides quantitative substrates of post-traumatic brain injury attention deficits in children. *Brain Connect.* 11 (8), 651–662. <https://doi.org/10.1089/brain.2020.0866>.
- Chamoun, R., Suki, D., Gopinath, S.P., Clay Goodman, J., Robertson, C., 2010. Role of extracellular glutamate measured by cerebral microdialysis in severe traumatic brain injury. *J. Neurosurg.* 113 (3), 564–570. <https://doi.org/10.3171/2009.12.JNS09689>.
- Chen, R.H., Ito, T., Kulkarni, K.R., Cole, M.W., 2018. The human brain traverses a common activation-pattern state space across task and rest. *Brain Connect.* 8 (7), 429–443. <https://doi.org/10.1089/brain.2018.0586>.
- Chiou, K.S., Jiang, T., Chiaravalloti, N., Hoptman, M.J., DeLuca, J., Genova, H., 2019. Longitudinal examination of the relationship between changes in white matter organization and cognitive outcome in chronic TBI. *Brain Inj.* 33 (7), 846–853. <https://doi.org/10.1080/02699052.2019.1606449>.
- Cohen, J.R., D'Esposito, M., 2016. The segregation and integration of distinct brain networks and their relationship to cognition. *J. Neurosci.* 36 (48), 12083–12094. <https://doi.org/10.1523/JNEUROSCI.2965-15.2016>.
- Cole, M.W., Pathak, S., Schneider, W., 2010. Identifying the brain's most globally connected regions. *Neuroimage* 49 (4), 3132–3148. <https://doi.org/10.1016/j.neuroimage.2009.11.001>.
- Cornblath, E.J., Ashourvan, A., Kim, J.Z., Betzel, R.F., Ciric, R., Adebimpe, A., Baum, G. L., et al., 2020. Temporal sequences of brain activity at rest are constrained by white matter structure and modulated by cognitive demands. *Commun. Biol.* 3 (1), 261. <https://doi.org/10.1038/s42003-020-0961-x>.
- Damoiseaux, J.S., Beckmann, C.F., Sanz Arigita, E.J., Barkhof, F., Scheltens, Ph., Stam, C. J., Smith, S.M., Rombouts, S.A.R.B., 2008. Reduced resting-state brain activity in the 'default network' in normal aging. *Cerebral Cortex (New York, N.Y.: 1991)* 18 (8), 1856–1864. <https://doi.org/10.1093/cercor/bhm207>.
- Delgado-Bonal, A., Marshak, A., 2019. Approximate entropy and sample entropy: a comprehensive tutorial. *Entropy* 21 (6), 541. <https://doi.org/10.3390/e21060541>.
- Dever, A., Powell, D., Graham, L., Mason, R., Das, J., Marshall, S.J., Vitorio, R., Godfrey, A., Stuart, S., 2022. Gait impairment in traumatic brain injury: a systematic review. *Sensors (Basel, Switzerland)* 22 (4), 1480. <https://doi.org/10.3390/s22041480>.
- Dixon, K.J., 2017. Pathophysiology of traumatic brain injury. *Phys. Med. Rehabil. Clin. N. Am.* 28 (2), 215–225. <https://doi.org/10.1016/j.pmr.2016.12.001>.
- Fan, J., McCandliss, B.D., Sommer, T., Raz, A., Posner, M.I., 2002. Testing the efficiency and independence of attentional networks. *J. Cogn. Neurosci.* 14 (3), 340–347. <https://doi.org/10.1162/089892902317361886>.
- Faul, M., Victor Coronado, 2015. "Epidemiology of Traumatic Brain Injury." In *Handbook of Clinical Neurology*, 127:3–13. Elsevier. <https://doi.org/10.1016/B978-0-444-52892-6.00001-5>.
- Fischl, B., 2012. FreeSurfer. *Neuroimage* 62 (2), 774–781. <https://doi.org/10.1016/j.neuroimage.2012.01.021>.
- Gardner, R.C., Yaffe, K., 2015. Epidemiology of mild traumatic brain injury and neurodegenerative disease. *Mol. Cell. Neurosci.* 66 (Pt B), 75–80. <https://doi.org/10.1016/j.mcn.2015.03.001>.
- Gentleman, S.M., Leclercq, P.D., Moyes, L., Graham, D.I., Smith, C., Griffin, W.S.T., Nicoll, J.A.R., 2004. Long-term intracerebral inflammatory response after traumatic brain injury. *Forensic Sci. Int.* 146 (2–3), 97–104. <https://doi.org/10.1016/j.forsciint.2004.06.027>.
- Glasser, M.F., Sotiroopoulos, S.N., Anthony Wilson, J., Coalson, T.S., Fischl, B., Andersson, J.L., Junqian, Xu, et al., 2013. The minimal preprocessing pipelines for the human connectome project. *Neuroimage* 80 (October), 105–124. <https://doi.org/10.1016/j.neuroimage.2013.04.127>.
- Gorgoraptis, N., Zaw-Linn, J., Feeney, C., Tenorio-Jimenez, C., Niemi, M., Malik, A., Ham, T., Goldstone, A.P., Sharp, D.J., 2019. Cognitive impairment and health-related quality of life following traumatic brain injury. *NeuroRehabilitation* 44 (3), 321–331. <https://doi.org/10.3233/NRE-182618>.
- Gu, S., Pasqualetti, F., Cieslik, M., Telesford, Q.K., Yu, A.B., Kahn, A.E., Medaglia, J.D., et al., 2015. Controllability of structural brain networks. *Nat. Commun.* 6 (1), 8414. <https://doi.org/10.1038/ncomms9414>.
- Gu, Z., Jamison, K.W., Sabuncu, M.R., Kuceyeski, A., 2021. Heritability and interindividual variability of regional structure-function coupling. *Nat. Commun.* 12 (1), 4894. <https://doi.org/10.1038/s41467-021-25184-4>.
- Guskiewicz, K.M., Broglio, S.P., 2015. Acute sports-related traumatic brain injury and repetitive concussion. *Handb. Clin. Neurol.* 127, 157–172. <https://doi.org/10.1016/B978-0-444-52892-6.00010-6>.
- Gutierrez-Barragan, D., Albert Basson, M., Panzeri, S., Gozzi, A., 2019. Infraslow state fluctuations govern spontaneous fMRI network dynamics. *Curr. Biol.* 29 (14), 2295–2306.e5. <https://doi.org/10.1016/j.cub.2019.06.017>.
- Hac, N.E.F., Gold, D.R., 2022. Neuro-visual and vestibular manifestations of concussion and mild TBI. *Curr. Opin. Neurol. Neurosci. Rep.* 22 (3), 219–228. <https://doi.org/10.1007/s11910-022-01184-9>.
- Harms, M.P., Somerville, L.H., Ances, B.M., Andersson, J., Barch, D.M., Bastiani, M., Bookheimer, S.Y., et al., 2018. Extending the human connectome project across ages: imaging protocols for the lifespan development and aging projects. *Neuroimage* 183 (December), 972–984. <https://doi.org/10.1016/j.neuroimage.2018.09.060>.
- He, X., Caciagli, L., Parkes, L., Stiso, J., Karrer, T.M., Kim, J.Z., Zhixin, Lu, et al., 2022. Uncovering the biological basis of control energy: structural and metabolic correlates of energy inefficiency in temporal lobe epilepsy. *Sci. Adv.* 8 (45), eabn2293. <https://doi.org/10.1126/sciadv.abn2293>.
- Howlett, J.R., Nelson, L.D., Stein, M.B., 2022. Mental health consequences of traumatic brain injury. *Biol. Psychiatry* 91 (5), 413–420. <https://doi.org/10.1016/j.biopsych.2021.09.024>.
- Imms, P., Clemente, A., Cook, M., D'souza, W., Wilson, P.H., Jones, D.K., Caeyenberghs, K., 2019. The structural connectome in traumatic brain injury: a meta-analysis of graph metrics. *Neurosci. Biobehav. Rev.* 99 (April), 128–137. <https://doi.org/10.1016/j.neubiorev.2019.01.002>.
- van der Horn, H.J., Liemburg, E.J., Aleman, A., Spikman, M.J., van der Naalt, J., 2015. Brain networks subserving emotion regulation and adaptation after mild traumatic brain injury. *J. Neurotrauma*. <https://doi.org/10.1089/neu.2015.3905>.
- Jacobs, M.L., Donders, J., 2007. Criterion validity of the California verbal learning test-second edition (CVLT-II) after traumatic brain injury. *Arch. Clin. Neuropsychol.* 22 (2), 143–149. <https://doi.org/10.1016/j.acn.2006.12.002>.
- Johnson, V.E., Stewart, J.E., Begbie, F.D., Trojanowski, J.Q., Smith, D.H., Stewart, W., 2013. Inflammation and white matter degeneration persist for years after a single traumatic brain injury. *Brain J. Neurol.* 136 (Pt 1), 28–42. <https://doi.org/10.1093/brain/aws322>.
- Karahanoglu, F.I., Van De Ville, D., 2015. Transient brain activity disentangles fMRI resting-state dynamics in terms of spatially and temporally overlapping networks. *Nat. Commun.* 6 (1), 7751. <https://doi.org/10.1038/ncomms8751>.
- Karrer, T.M., Kim, J.Z., Stiso, J., Kahn, A.E., Pasqualetti, F., Habel, U., Bassett, D.S., 2020. A practical guide to methodological considerations in the controllability of structural brain networks. *J. Neural Eng.* 17 (2), 026031. <https://doi.org/10.1088/1741-2552/ab6e8b>.
- Kuceyeski, A.F., Jamison, K.W., Owen, J.P., Raj, A., Mukherjee, P., 2019. Longitudinal increases in structural connectome segregation and functional connectome integration are associated with better recovery after mild TBI. *Hum. Brain Mapp.* 40 (15), 4441–4456. <https://doi.org/10.1002/hbm.24713>.
- Landeghem, F.K.H.V., Weiss, T., Oehmichen, M., von Deimling, A., 2006. Decreased expression of glutamate transporters in astrocytes after human traumatic brain injury. *J. Neurotrauma* 23 (10), 1518–1528. <https://doi.org/10.1089/neu.2006.23.1518>.
- Liu, X., Duyu, J.H., 2013. Time-varying functional network information extracted from brief instances of spontaneous brain activity. *PNAS* 110 (11), 4392–4437. <https://doi.org/10.1073/pnas.1216856110>.
- Lotocki, G., de Rivero Vaccari, J.P., Perez, E.R., Sanchez-Molano, J., Furones-Alonso, O., Bramlett, H.M., Dalton Dietrich, W., 2009. Alterations in blood-brain barrier permeability to large and small molecules and leukocyte accumulation after traumatic brain injury: effects of post-traumatic hypothermia. *J. Neurotrauma* 26 (7), 1123–1134. <https://doi.org/10.1089/neu.2008.0802>.

- Luppi, Andrea I., Parker Singleton, S., Justine Y. Hansen, Danilo Bzdok, Amy Kuceyeski, Richard F. Betzel, Bratislav Misic. 2023. "Transitions between Cognitive Topographies: Contributions of Network Structure, Neuromodulation, and Disease." bioRxiv. <https://doi.org/10.1101/2023.03.16.532981>.
- Machamer, J., Temkin, N., Dikmen, S., Nelson, L.D., Barber, J., Hwang, P., Boase, K., et al., 2022. Symptom frequency and persistence in the first year after traumatic brain injury: a TRACK-TBI study. *J. Neurotrauma* 39 (5–6), 358–370. <https://doi.org/10.1089/neu.2021.0348>.
- Margulies, D.S., Ghosh, S.S., Goulas, A., Falkiewicz, M., Hunttenburg, J.M., Langs, G., Bezgin, G., et al., 2016. Situating the default-mode network along a principal gradient of macroscale cortical organization. *Proc. Natl. Acad. Sci.* 113 (44), 12574–12579. <https://doi.org/10.1073/pnas.1608282113>.
- Mayer, A.R., Mannell, M.V., Ling, J., Gasparovic, C., Yeo, R.A., 2011. Functional connectivity in mild traumatic brain injury. *Hum. Brain Mapp.* 32 (11), 1825–1835. <https://doi.org/10.1002/hbm.21151>.
- McAllister, T., McCrea, M., 2017. Long-term cognitive and neuropsychiatric consequences of repetitive concussion and head-impact exposure. *J. Athl. Train.* 52 (3), 309–317. <https://doi.org/10.4085/1062-6050-52.1.14>.
- McNamee, S., Walker, W., Cifu, D.X., Wehman, P.H., 2009. Minimizing the effect of TBI-related physical sequelae on vocational return. *J. Rehabil. Res. Dev.* 46 (6), 893–908. <https://doi.org/10.1682/jrrd.2008.08.0106>.
- Meningher, I., Bernstein-Eliav, M., Rubovitch, V., Pick, C.G., Tavor, I., 2020. Alterations in network connectivity after traumatic brain injury in mice. *J. Neurotrauma* 37 (20), 2169–2179. <https://doi.org/10.1089/neu.2020.7063>.
- Moretto, M., Silvestri, E., Zangrossi, A., Corbetta, M., Bertoldo, A., 2022. Unveiling whole-brain dynamics in normal aging through hidden markov models. *Hum. Brain Mapp.* 43 (3), 1129–1144. <https://doi.org/10.1002/hbm.25714>.
- Ng, S.Y., Lee, A.Y.W., 2019. Traumatic brain injuries: pathophysiology and potential therapeutic targets. *Front. Cell. Neurosci.* 13, 528. <https://doi.org/10.3389/fncel.2019.00528>.
- Nieto-Castanon, A., Whitfield-Gabrieli, S., 2021. *CONN Functional Connectivity Toolbox: RRID SCR_009550, Release 21*, twentyfirst ed. Hilbert Press.
- Olafson, E., Russello, G., Jamison, K.W., Liu, H., Wang, D., Bruss, J.E., Boes, A.D., Kuceyeski, A., 2022. Frontoparietal network activation is associated with motor recovery in ischemic stroke patients. *Commun. Biol.* 5 (1), 1–11. <https://doi.org/10.1038/s42003-022-03950-4>.
- Padula, W.V., Capo-Aponte, J.E., Padula, W.V., Singman, E.L., Jenness, J., 2017. The consequence of spatial visual processing dysfunction caused by traumatic brain injury (TBI). *Brain Inj.* 31 (5), 589–600. <https://doi.org/10.1080/02699052.2017.1291991>.
- Palacios, E.M., Yuh, E.L., Chang, Y.-S., Yue, J.K., Schnyer, D.M., Okonkwo, D.O., Valadka, A.B., et al., 2017. Resting-state functional connectivity alterations associated with six-month outcomes in mild traumatic brain injury. *J. Neurotrauma* 34 (8), 1546–1557. <https://doi.org/10.1089/neu.2016.4752>.
- Park, H.-J., Friston, K., 2013. Structural and functional brain networks: from connections to cognition. *Science* 342 (6158), 1238411. <https://doi.org/10.1126/science.1238411>.
- Parkes Linden, Jason Z. Kim, Jennifer Stiso, Julia K. Brynildsen, Matthew Cieslak, Sydney Covitz, Raquel E. Gur, et al., 2023. "Using Network Control Theory to Study the Dynamics of the Structural Connectome." bioRxiv. <https://doi.org/10.1101/2023.08.23.554519>.
- Parkes, L., Kim, J.Z., Stiso, J., Calkins, M.E., Cieslak, M., Gur, R.E., Gur, R.C., et al., 2022. Asymmetric signaling across the hierarchy of cytoarchitecture within the human connectome. *Sci. Adv.* 8 (50), eadd2185. <https://doi.org/10.1126/sciadv.add2185>.
- Petraglia, A.L., Plog, B.A., Dayawansa, S., Chen, M., Dashnow, M.L., Czerniecka, K., Walker, C.T., et al., 2014. The spectrum of neurobehavioral sequelae after repetitive mild traumatic brain injury: a novel mouse model of chronic traumatic encephalopathy. *J. Neurotrauma* 31 (13), 1211–1224. <https://doi.org/10.1089/neu.2013.3255>.
- Povlishock, J.T., 1992. Traumatically induced axonal injury: pathogenesis and pathobiological implications. *Brain Pathol. (Zurich, Switzerland)* 2 (1), 1–12.
- Power, J.D., Mitra, A., Laumann, T.O., Snyder, A.Z., Schlaggar, B.L., Petersen, S.E., 2014. Methods to detect, characterize, and remove motion artifact in resting state fMRI. *Neuroimage* 84 (January), 320–341. <https://doi.org/10.1016/j.neuroimage.2013.08.048>.
- Power, J.D., Schlaggar, B.L., Lessov-Schlaggar, C.N., Petersen, S.E., 2013. Evidence for hubs in human functional brain networks. *Neuron* 79 (4), 798–813. <https://doi.org/10.1016/j.neuron.2013.07.035>.
- Rao, V., Lyketsos, C., 2000. Neuropsychiatric sequelae of traumatic brain injury. *Traum. Brain Inj.*
- Shafer, A.T., Beason-Held, L., An, Y., Williams, O.A., Huo, Y., Landman, B.A., Caffo, B.S., Resnick, S.M., 2021. Default mode network connectivity and cognition in the aging brain: the effects of age, sex, and APOE genotype. *Neurobiol. Aging* 104 (August), 10–23. <https://doi.org/10.1016/j.neurobiolaging.2021.03.013>.
- Silverberg, N.D., Iaccarino, M.A., Panenka, W.J., Iverson, G.L., McCulloch, K.L., Dams-O'Connor, K., Reed, N., McCrea, M., American Congress of Rehabilitation Medicine
- Brain Injury Interdisciplinary Special Interest Group Mild TBI Task Force, 2020. Management of concussion and mild traumatic brain injury: a synthesis of practice guidelines. *Arch. Phys. Med. Rehabil.* 101 (2), 382–393. <https://doi.org/10.1016/j.apmr.2019.10.179>.
- Singleton, S.P., Luppi, A.I., Carhart-Harris, R.L., Cruzat, J., Roseman, L., Nutt, D.J., Deco, G., Kringelbach, M.L., Stamatakis, E.A., Kuceyeski, A., 2022. Receptor-informed network control theory links LSD and psilocybin to a flattening of the brain's control energy landscape. *Nat. Commun.* 13 (1), 5812. <https://doi.org/10.1038/s41467-022-33578-1>.
- Singleton, S., Parker, Christopher Timmermann, Andrea I. Luppi, Emma Eckernäs, Leon Roseman, Robin L. Carhart-Harris, Amy Kuceyeski. 2023. "Time-Resolved Network Control Analysis Links Reduced Control Energy under DMT with the Serotonin 2a Receptor, Signal Diversity, and Subjective Experience." bioRxiv: The Preprint Server for Biology, May, 2023.05.11.540409. <https://doi.org/10.1101/2023.05.11.540409>.
- Singleton, S., Parker, Puneet Velidi, Louisa Schilling, Andrea I. Luppi, Keith Jamison, Linden Parkes, and Amy Kuceyeski. 2023. "Altered Structural Connectivity and Functional Brain Dynamics in Individuals with Heavy Alcohol Use." bioRxiv. <https://doi.org/10.1101/2023.11.27.568762>.
- Spreng, R.N., Turner, G.R., 2013. Structural covariance of the default network in healthy and pathological aging. *J. Neurosci.* 33 (38), 15226–15234. <https://doi.org/10.1523/JNEUROSCI.2261-13.2013>.
- Sun, Yu., Yin, Q., Fang, R., Yan, X., Wang, Y., Bezerianos, A., Tang, H., Miao, F., Sun, J., 2014. Disrupted functional brain connectivity and its association to structural connectivity in amnestic mild cognitive impairment and Alzheimer's disease. *PLoS One* 9 (5), e96505. <https://doi.org/10.1371/journal.pone.0096505>.
- Tomasi, D., Volkow, N.D., 2012. Functional connectivity density and the aging brain. *Mol. Psychiatry* 17 (5), 471. <https://doi.org/10.1038/mp.2012.27>.
- Tomčala, J., 2020. New fast ApEn and SampEn entropy algorithms implementation and their application to supercomputer power consumption. *Entropy* 22 (8), 863. <https://doi.org/10.3390/e22080863>.
- Tournier, J.-D., Calamante, F., Connelly, A., 2012. Mrtrix: diffusion tractography in crossing fiber regions. *Int. J. Imaging Syst. Technol.* 22 (1), 53–66. <https://doi.org/10.1002/ima.22005>.
- Tozlu, C., Card, S., Jamison, K., Gauthier, S.A., Kuceyeski, A., 2023. Larger lesion volume in people with multiple sclerosis is associated with increased transition energies between brain states and decreased entropy of brain activity. *Netw. Neurosci. (Cambridge, Mass.)* 7 (2), 539–556. https://doi.org/10.1162/netn_a_00292.
- Vanitallie, T.B., 2019. Traumatic brain injury (TBI) in collision sports: possible mechanisms of transformation into chronic traumatic encephalopathy (CTE). *Metab. Clin. Exp.* 1005 (November), 153943. <https://doi.org/10.1016/j.metabol.2019.07.007>.
- Varangis, E., Habeck, C.G., Razlighi, Q.R., Stern, Y., 2019. The effect of aging on resting state connectivity of predefined networks in the brain. *Front. Aging Neurosci.* 11, 234. <https://doi.org/10.3389/fnagi.2019.00234>.
- Vidaurre, D., Smith, S.M., Woolrich, M.W., 2017. Brain network dynamics are hierarchically organized in time. *PNAS* 114 (48), 12827–12832. <https://doi.org/10.1073/pnas.1705120114>.
- Wang, S., Gan, S., Yang, X., Li, T., Xiong, F., Jia, X., Sun, Y., Liu, J., Zhang, M., Bai, L., 2021. Decoupling of structural and functional connectivity in hubs and cognitive impairment after mild traumatic brain injury. *Brain Connect.* 11 (9), 745–758. <https://doi.org/10.1089/brain.2020.0852>.
- Wang, Y., Vlemincx, E., Vantieghem, I., Dhar, M., Dong, D., Vandekerckhove, M., 2022. Bottom-up and cognitive top-down emotion regulation: experiential emotion regulation and cognitive reappraisal on stress relief and follow-up sleep physiology. *Int. J. Environ. Res. Public Health* 19 (13), 7621. <https://doi.org/10.3390/ijerph19137621>.
- Wang, Z., Li, Y., Childress, A.R., Detre, J.A., 2014. Brain entropy mapping using fMRI. Edited by Satoru Hayasaka. *PLoS One* 9 (3), e89948. <https://doi.org/10.1371/journal.pone.0089948>.
- Xiong, Y., Gu, Q., Peterson, P.L., Muizelaar, J.P., Lee, C.P., 1997. Mitochondrial dysfunction and calcium perturbation induced by traumatic brain injury. *J. Neurotrauma* 14 (1), 23–34. <https://doi.org/10.1089/neu.1997.14.23>.
- Yeo, B.T., Thomas, F.M., Krienen, J.S., Sabuncu, M.R., Lashkari, D., Hollinshead, M., Roffman, J.L., et al., 2011. The organization of the human cerebral cortex estimated by intrinsic functional connectivity. *J. Neurophysiol.* 106 (3), 1125–1165. <https://doi.org/10.1152/jn.00338.2011>.
- Yuan, W., Wade, S.L., Quatman-Yates, C., Hugentobler, J.A., Gubanich, P.J., Kurowski, B. G., 2017. Structural connectivity related to persistent symptoms after mild TBI in adolescents and response to aerobic training: preliminary investigation. *J. Head Trauma Rehabil.* 32 (6), 378–384. <https://doi.org/10.1097/HTR.0000000000000318>.
- Zonneveld, H.I., Pruijm, R.H., Bos, D., Vrooman, H.A., Muetzel, R.L., Hofman, A., Rombouts, S.A., et al., 2019. Patterns of functional connectivity in an aging population: the Rotterdam study. *Neuroimage* 189 (April), 432–444. <https://doi.org/10.1016/j.neuroimage.2019.01.041>.